Measurement of Macro- and Microstress of Dual Phase Composite Materials by X-Ray Diffraction Method Using Imaging Plate

Measurement of Macro- and Microstresses of Dual Phase Composite Materials by X-Ray Diffraction Method Using Imaging Plate

Toshihiko SASAKI and Shigeki TAKAGO*

Abstract

A newly developed method for the x-ray stress analysis was studied. This method is not a ψ-angle based method which the conventional x-ray methods usually use, but a α-angle based one, where ψ is the angle between the normals of both the lattice plane and the sample and α is the angle at the circumference of the Debye-Scherrer ring. The use of the α-angle based method allows to obtain stresses by the single x-ray incidence method using the whole part of the Debye-Scherrer ring detected with an area detector. Since it is possible to detect each Debye-Scherrer rings diffracted from each constituents of the material at the same time because the diffraction rings usually possess the different radius each other due to the different diffraction angle, such nature allows to measure all of the phase stresses (mean stresses in the constituent) at the same time. It is, therefore, expected that the measurement of the macro- and microstresses becomes to be much quicker than a case of the use of the conventional $\sin^2\psi$ method (ψ-angle based method). In this study, the stress measurement mentioned above was carried out for a dual phase stainless steel. In case of the use of chromium x-ray radiation to this material, the 211 diffraction of the α-phase occurs at $2\theta=153.5$ deg. by Kα radiation, where θ is Bragg's angle, and 220 diffraction of the γ-phase does at $2\theta=128.9$ deg. by K α radiation. The experiment of the measurement of the phase stresses in the specimen under the mechanical loading using a four-point bending device is shown. The results are discussed by comparing with those obtained by the conventional method as well as with the theoretical simulation using the Eshelby's approach. It is shown that the accuracy of the present method is almost the same as that of the conventional one.

Introduction

The x-ray diffraction technique is useful for determining the actual state of the stress in the material, especially in the composite materials. This is because the method allows to obtain not only the mean stresses (phase stresses) in each constituents, but also the macroscopic stress (macrostress) in the overall diffraction volume and the microscopic stress (microstress). In case of the other experimental method, for example, the magnetic method or that using

平成9年9月12日受理

* *Graduate School of Education, Kanazawa Univ., Kakuma, Kanazawa 920-11, Japan.*

ultrasonic, it is usually very difficult to carry out the similar stress measurement.

In the conventional method of the x-ray stress analysis, the so-called $\sin^2\psi$ method is used as a principle of the stress calculation, and the 0-d or 1-d x-ray detector is also used. Beside of many advantages in the method, there is a problem that the experiment consumes longer time when the state of the stress in the material is complicated, for example, triaxial stress, steep stress gradient and microscopic stress. The use of 1-d x-ray detectors such as a position sensitive proportional counter (PSPC) is effective to this problem. However, the fact that we need to measure a lot of diffraction data, for example, many lattice strains in different ψ-tilts and ϕ-atomize angles does not change by the use of a PSPC.

The use of a 2-d detector is effective to obtain a lot of diffraction data at the same time, so that it can be a solution to shorten the time needed in the x-ray measurement. Moreover, the use of the as a principle for the stress determination instead of the conventional ψ-angle based method (the $\sin^2\psi$ method) would also be effective for this purpose. In this study, the imaging-plate (IP) was used as a 2-d detector and the $\cos\alpha$ method, which was proposed by Taira et al. in 1978 and belongs to the α-angle based method, was adopted as a principle for the stress determination. The study on the x-ray stress measurement using both an IP and the $\cos\alpha$ method has been already done by Yoshioka et al. So, the purpose of this study is to analyze macro- and microstresses in composite materials at the same time. Since it is possible to detect each Debye-Scherrer rings diffracted from each constituents of the material at the same time because the diffraction rings usually possess the different radius each other due to the different diffraction angle, such nature allows to measure all of the phase stresses (mean stresses in the constituent) at the same time. It is, therefore, expected that the measurement of the macro- and microstresses becomes to be much quicker than a case of the use of the conventional $\sin^2\psi$ method. An experiment was made with the specimen of ferritic and austenitic stainless steel (SUS329J4L). The stress analysis was done for the case of both the mechanical loading and the residual stress state. The results were compared with those which were obtained using the conventional method, and also with theoretical values which were obtained based on the Eshelby's approach.

Theory

Principle for determining phase stresses using whole circumference of one Debye-Scherrer ring (the Cosα method)

Consider a diffraction ring which emerged from the material when the orientation of the incidence x-ray beam is expressed by ϕ_0 and ψ_0 as shown in Fig. 1. Direction cosines, n_{3i} ($i=1, 2, 3$), of the normal (L_3 axis) of the lattice plane of crystals which satisfies the diffraction condition (the Bragg's law) are written as

$$\left.\begin{aligned} n_{31}&=\cos\eta\sin\psi_0-\sin\eta\cos\psi_0\cos\alpha \\ n_{32}&=\sin\eta\sin\alpha \\ n_{33}&=\cos\eta\sin\psi_0+\sin\eta\sin\psi_0\cos\alpha \end{aligned}\right\} \quad \cdots\cdots(1)$$

where η is a supplementary angle of 2θ and α is the angle at the circumference. We write S_i for the sample coordinate system, and L_i for the laboratory coordinate system which can be obtained by rotating S_i as to coincide L_3 to the direction parallel to n_{3i}. Denoting the normal strain ε_{33}^{L} in a direction of L_3 by ε_α, we have

$$\varepsilon_\alpha=\varepsilon_{33}^{\alpha}=n_{3i}n_{3j}\varepsilon_{ij}^{S} \quad \cdots\cdots(2)$$

where ε_{ij}^{S} is the strains in S_i system and have relation to the stresses σ_{ij}^{S} in S_i system as below

$$\varepsilon_{ij}^{S}=\left(\frac{s_2}{2}\right)\sigma_{ij}^{S}+\sigma(s_1)(\sigma_{11}^{S}+\sigma_{22}^{S}+\sigma_{33}^{S}) \quad \cdots\cdots(3)$$

where s_1 and s_2 are the x-ray elastic constants and have the following relations using Young's modulus (E) and Poisson's ratio (ν) respectively.

$$s_1=-\frac{\nu}{E},\ \frac{s_2}{2}=\frac{1+\nu}{E} \quad \cdots\cdots(4)$$

Consider four strains which can be obtained from the same diffraction ring having the different angles at the circumference as α, $-\alpha$, $\pi+\alpha$ and $\pi-\alpha$ as shown in Fig. 2, and denote them as ε_α, $\varepsilon_{-\alpha}$, $\varepsilon_{\pi+\alpha}$ and $\varepsilon_{\pi-\alpha}$. From these strains we define the following new parameter a_1

$$a_1\equiv\frac{1}{2}[(\varepsilon_\alpha-\varepsilon_{\pi+\alpha})+(\varepsilon_{-\alpha}-\varepsilon_{\pi-\alpha})] \quad \cdots\cdots(5)$$

Expressing eqn(5) in terms of stresses in S_i coordinate using eqns(1)~(3), we have

$$a_1=-\left(\frac{s_2}{2}\right)[(\sigma_{11}-\sigma_{33})\sin2\psi_0 +2\sigma_{13}\cos2\psi_0]\sin2\eta\cos\alpha \quad \cdots\cdots(6)$$

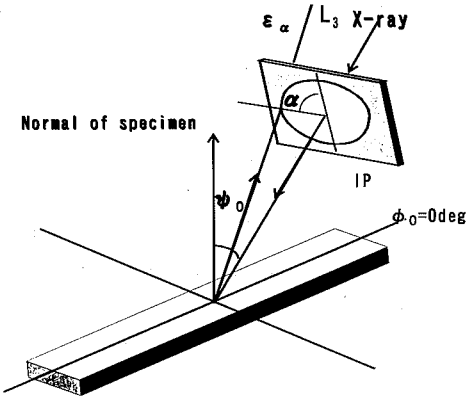

Fig. 1 Schematic view of optics for the α-angle based x-ray stress analysis and definitions of coordinate systems and symbols used in the text.

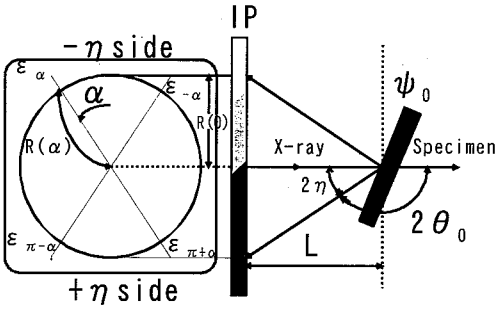

Fig. 2 Principle of cosα method for determining stress using x-ray strains obtained from one diffraction ring.

where symbol S, which expresses the sample coordinate system, was abbreviated here. As it is reasonable to assume that $\sigma_{13}=\sigma_{23}=0$ in the practical use, the following argument will be made under this assumption. Consequently, from eqn(6) we have

$$\sigma_{11}-\sigma_{33}=-\left(\frac{2}{s_2}\right)\frac{1}{\sin 2\eta}\frac{1}{\sin 2\psi_0}\left(\frac{\partial a_1}{\partial \cos\alpha}\right) \quad \cdots\cdots(7)$$

We can see that one can obtain stress $(\sigma_{11}-\sigma_{33})$ using eqn(7) from the slope in the relation between a_1 vs. $\cos\alpha$, which can be derived from a single diffraction ring recorded on IP. Selecting an adequate condition of x-ray diffraction, one would be able to record both diffraction rings emerged from matrix and the second phase on one IP at the same time. In such case, we can obtain each phase stresses in the both constituents in the material at the same time. Noyan et al.[3]~[7] developed the method for determining the macro- and microstresses from the phase stresses in all constituents, which will be explained briefly in the next section.

Determination of Macro- and Microstresses

When an external stress is applied to a composite material, a microscopic stress state, as shown in Fig. 3, is usually built up in the composite material due to the misfit of mechanical properties between the constituents. The following equations can be deduced from the equilibrium condition of microstresses.

$$\left.\begin{aligned}(\sigma_{11}^{M}-\sigma_{33}^{M})&=(\sigma_{11}^{0}-\sigma_{33}^{0})+(\sigma_{11}^{m}-\sigma_{33}^{m})\\(\sigma_{11}^{I}-\sigma_{33}^{I})&=(\sigma_{11}^{0}-\sigma_{33}^{0})+(\sigma_{11}^{\Omega}-\sigma_{33}^{\Omega})\\(\sigma_{11}^{0}-\sigma_{33}^{0})&=(1-f)(\sigma_{11}^{M}-\sigma_{33}^{M})+f(\sigma_{11}^{I}-\sigma_{33}^{I})\end{aligned}\right\}\quad(8)$$

where σ^{m} and σ^{Ω} are the microstresses in the matrix and the second phase respectively, σ^{M}, σ^{I} are the phase stresses in the matrix and the second phase, and f is the volume fraction of the second phase. From these equations we have

$$\left.\begin{aligned}(\sigma_{11}^{m}-\sigma_{33}^{m})&=f[(\sigma_{11}^{M}-\sigma_{33}^{M})-(\sigma_{11}^{I}-\sigma_{33}^{I})]\\(\sigma_{11}^{\Omega}-\sigma_{33}^{\Omega})&=(f-1)[(\sigma_{11}^{M}-\sigma_{33}^{M})-(\sigma_{11}^{I}-\sigma_{33}^{I})]\end{aligned}\right\}\quad(9)$$

which enables us to obtain the macro- and microstresses in the material if phase stresses in all constituents are found.

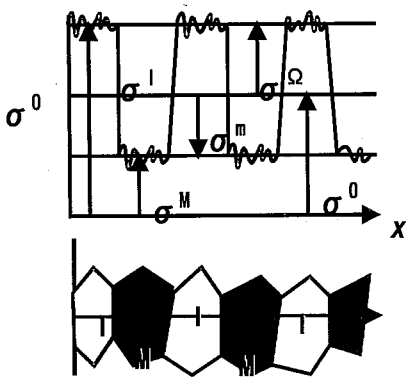

Fig. 3　Schematic illustration for macro- and microstresses built up in composite materials due to misfit strain between matrix and inhomogeneous inclusions.

Experimental

Materials and Specimen

Ferritic (α) and austenitic (γ) dual phase stainless steel (JIS-SUS329J4L), which was manufactured by a continuous casting process, was used in the experiment. The chemical components and mechanical properties were shown in Table 1 and 2 respectively. Specimens used in the experiment were fabricated through the process of cutting from a rolled plate of the size of the length of 1524mm, the thickness of 6mm and the width of 300mm, and then milling and grinding. The final configuration of the specimen was as the length of 60mm, the thickness of 5mm and the width of 10mm respectively. The longitudinal direction of the specimen was coincided to the rolling direction. The specimens were quenched in water after keeping at 1373K for 60min. The surface of the specimens was polished by means of emery paper.

Conditions for X-ray Diffraction

The changes in each phase stresses in α and γ phases of the dual phase stainless steel were measured under the applied stress using the four-point-bending device shown in Fig. 4. Conditions for the x-ray diffraction experiment used are summarized in Table 3. The applied stress was monitored by means of a strain gauge bonded at the surface of the specimen opposite to x-ray irradiated one. The applied strain was ranged from 0 to 1000×10^{-6} with an interval of 250×10^{-6}.

Cr-Kα radiation was used under the tube voltage of 30kV and the tube current of 10mA. The diameter of the collimator used was 1mm. The incidence angle of the x-ray beams was $\psi_0=30°$. An IP sheet of 5in×5in, which was set in the x-ray camera based on Laue method, was used. The IP read-out system, which is on the market (Rigaku), was used in order to store the digital image data of diffraction images into the computer. In the system, the IP sheet is put on the drum which rotates during read-out time, and is irradiated by the He-Ne laser beam. The diffraction intensity was analyzed by means of the intensity of the light illuminated from

Table 1 Chemical composition of SUS329J4L. (wt.%)

C	Si	Mn	P	S	Cr	Ni	Mo	Cu	W	N
0.016	0.5	0.91	0.02	0.002	24.67	7.37	3.01	0.43	0.29	0.16

Table 2 Mechanical properties of SUS329J4L.

Yield strength, MPa	598
Tensile strength, MPa	778
Elongation, %	39
Reduction of area, %	71
γ -phase volume fraction , %	50
Young's modulus, GPa	199.4

IP after this process. The resolution of the intensity distribution was 100μm. Then, the diffraction ring image was expressed by the digital data consisted of 1150×1140 pixels. The location of the incidence x-ray beam on the IP image was roughly determined from the display of the computer. The location was used as an initial one for the precise determination which is explained in ref.(8). The diffraction profiles were obtained as the distributions of the diffraction intensity along the radial direction of the diffraction ring from the location of the incidence beam determined above. These profiles were derived from $\alpha=0$ to $\alpha=359$ deg. with the interval of 1 deg.

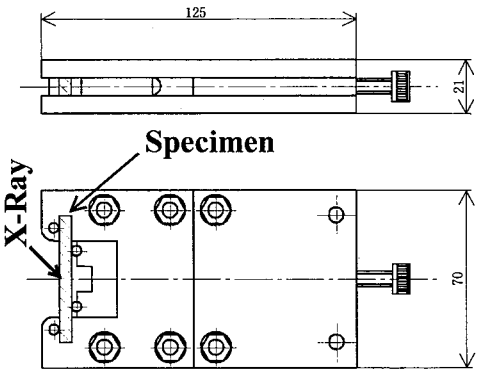

Fig. 4　Device used for four-point-bending test.

Results and Discussion

Debye-Scherrer Rings and Diffraction Profiles

Fig. 5(a) shows an example of the diffraction rings obtained from the specimen using Cr-Kα radiation. The diffraction ring was obtained carrying out the sample plane oscillation method which was discussed in ref.(9). They shows continuous and uniformly distribution of the

Table 3　Conditions of x-ray diffraction experiment for dual phase stainless steel.

	Ferrite	Austenite
Characteristic X-ray	Cr	Cr
Diffraction	α 211	γ 220
Filter	V	V
Tube voltage, kV	30	30
Tube current, mA	50	50
Exposure time(Specimen), sec.	180	180
Incidence angle, deg	30	30
Camera length, mm	35	35
Diffraction angle, deg	153.54	128.9
Peak position	Half value breadth method	Half value breadth method
Mechanical Young's modulus, GPa	206	193
Mechanical Poisson's ratio	0.28	0.30
X-ray elastic constant ,GPa	175	149

intensity. This means that the grain size in the specimen is relatively small and there are many grains within the diffraction volume, so that the x-ray stress measurement can be made successively. Though the broadening can be seen in the diffraction profiles, it is not a serious state for x-ray stress analysis. Fig. 5(b) shows diffraction profiles for four different angles α obtained from the diffraction ring data shown in Fig. 5(a) by means of image processing method developed in this study. As shown in the figure, both peaks for the α and the γ phases were detected on an IP at the same time. The reason why the intensity is weak around $\phi=270$ deg. is the x-ray absorption due to the increase of the tilt of the diffraction beams from the normal of the specimen, as well as to the decrease of the number of grains diffracting due to the existence of the rolling texture.

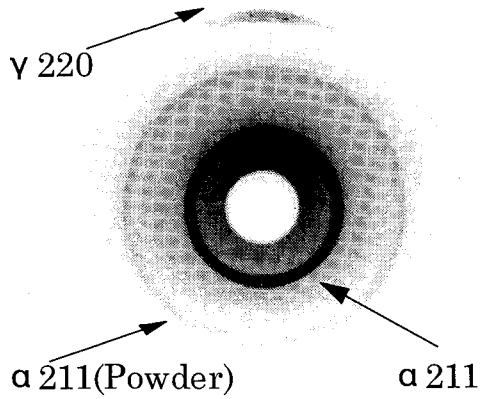

(a)

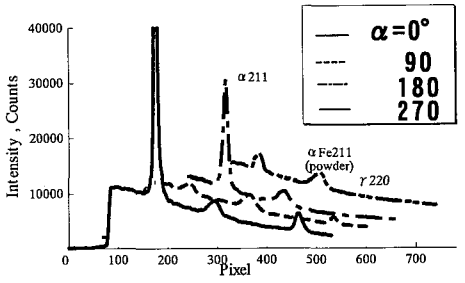

(b)

Fig. 5 Photograph of a diffraction ring obtained from the specimen (a), and its diffraction profiles for $\alpha=0$, 90, 180, 270 deg (b).

Determination of Stress

Fig. 6 shows the distribution of the peak positions determined from each diffraction profiles. The inner plots in the figure correspond to the α211 diffraction and the outer ones to the γ220 diffraction respectively. The peak determination was carried out after processing image data such as the software oscillation method, which is explained in ref.(8), as well as the smoothing treatment to the diffraction profiles.

Fig. 7 shows the a_1 vs. $\cos\alpha$ plots written by eqn(5). It is shown in the figure that each plots show linear relations as being expected from eqn(6), and also that the slopes in these plots decreases due to the increase of the applied stress. Applying eqn(7) to the data of Fig. 7, the phase stresses were calculated, and then the macro- and microstresses were also done using eqn (9). Here, the x-ray elastic constants used were cited from the literature, that is, those of the α phase were the data obtained from steel and those of the γ phase were from an austenitic stainless steel. Fig. 8 shows the relation between each stresses obtained by this manner and applied stresses. The lines in the figures show the relation obtained using the theoretical equation called the Eshelby/Mori-Tanaka method. The theory, however, can estimate only the

slope of the relation but not the intersection (namely, residual stress). So the theoretical lines were drawn as to fit to data, keeping the slope to be the theoretical value. At the calculation of the theoretical values, it is assumed that $\sigma_{33}^{0}=0$ since at the experiment the load was applied in an uni-axial. From Fig. 8, we can see that the slope between the phase stress for the α phase and the applied stress is a bit larger than that of the γ phase, which almost agrees with the theoretical value. The similar tendency can be seen in the figure showing the result on the microstresses (Fig. 8(b)). These all results show the validity of the present method for determining macro- and microstresses.

Conclusions

The method for determining stress using the α-angle based method was investigated for the case of the microscopic stress analysis by use of an imaging-plate (IP). In this study, this method was used to measure the phase stresses, macro- and microstresses in both constituents in the two phase stainless steel at the same time

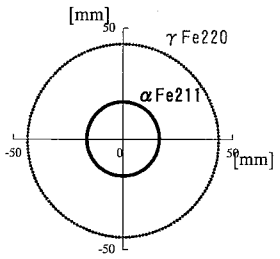

Fig. 6　Distribution of peak positions obtained from diffraction ring.

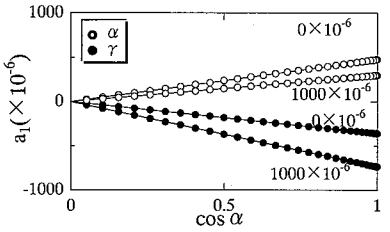

Fig. 7　Experimental result on the parameter a_1, which is explained in eq. (5) in the text, as a function of cosα.

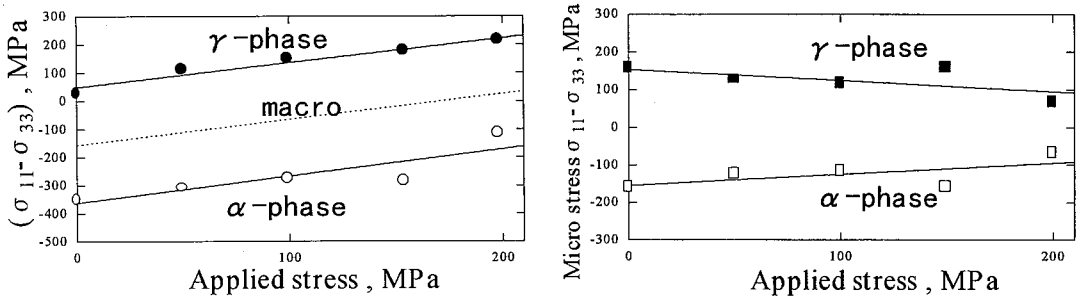

Fig. 8　Results of the stress measurement during bending test. Left figure shows the phase stresses and macrostresses as a function of applied stress. Right one shows similar relation on microstresses.

by the single incidence x-ray method. The stresses obtained in this study agreed well with theoretical ones which was based on the Eshelby's approach.

References

1) Hanabusa,T. and Fujiwara,H., 32nd Jpn.Congr. Mat.Res., 27(1989).
2) Tanaka,K. Mine,T. Suzuki,K. *The Society of Materials Science*, **39**−444, 1235 (1990).
3) Noyan,I.,C.,Met.Trans., **A14**, 1907 (1983).
4) Predecki,P.,K. et.al., Adv. X-ray Anal., **31**, 231 (1988).
5) Hauk,V. and Oudelhoven,R.,Z.Metallkde, **79**, 41 (1988).
6) Amemiya, Y., et. al., *The Japan. Society Applied Physics*, **55**,957 (1986).
7) Amemiya,Y., Kamiya,N. and Satow,Y.,Nucl. Instr. and Meth. **A246**, 572 (1986).
8) Sasaki, T. and Hirose, Y. *Journal of the Japan Society of Mechanical and Engineers*, **61**−590, A180 (1995).
9) Sasaki, T. Hirose, Y. and Yasukawa, S., *Journal of the Japan Society of Mechanical and Engineers*, **63**−607, A533 (1997).
10) *X-ray stress measurement standard, The Society of Materials Science* (1982).
11) Eshelby,J.,D.,Proc. R. Soc. London, **A241**, 379 (1957).
12) Mori,T. and Tanaka,K.,Acta Metall., **21**, 571 (1973).
13) Lin,S.,C.,Yang,C.,C.,Mura,T. and Iwakuma,T., Int.J. Solids Structures, **29-14/15**, 1859 (1992).
14) Sasaki,T., Lin, Z., and Hirose, Y., *Journal of the Japan Society of Mechanical and Engineers*, **63**, No. 606. 370 (1997).